

## 3d transition metal impurities in aluminum: A first-principles study

M. Mantina, S. L. Shang, Y. Wang, L. Q. Chen, and Z. K. Liu

*Department of Materials Science and Engineering, The Pennsylvania State University, University Park, Pennsylvania 16802, USA*

(Received 28 March 2009; revised manuscript received 9 September 2009; published 18 November 2009)

In this work, appropriate description of interactions of 3d transition metals in aluminum (Al-3d) is attained from first-principles using LDA+*U* potential within density-functional theory. By reproducing diffusion coefficients of 3d transition metals in aluminum in agreement with reliable data from experiments, activation energies, and diffusion prefactors along with different aspects of the Al-3d systems are presented. Al alloy with dilute concentration of 3d solutes Fe, Cr, or Mn is magnetic. The physics underlying the anomalously low diffusivities of 3d solutes in Al is discussed.

DOI: [10.1103/PhysRevB.80.184111](https://doi.org/10.1103/PhysRevB.80.184111)

PACS number(s): 66.30.J–

### I. INTRODUCTION

Aluminum alloys with 3d transition metal elements are important commercial alloys. During the last decade, first-principles calculations<sup>1–5</sup> have been employed to study diffusion in dilute Al-3d alloy systems. Simonovic *et al.*<sup>1</sup> estimated activation energies in Al for several elements including the 3d elements using generalized gradient approximation while Sandberg *et al.*<sup>2</sup> predicted diffusion barriers of 3d impurities in Al using local-density approximation (LDA), within density-functional theory (DFT). Researchers<sup>3–5</sup> have also specifically investigated the magnetic property of 3d elements in Al using *ab initio* procedures. Sensitivity of migration barriers<sup>2,4</sup> and local magnetic moments<sup>3–5</sup> of the 3d impurities to the geometry of the initial system configuration and the extent of relaxation is reported. The present work is aimed at obtaining diffusivities of 3d solutes in Al by calculating both the diffusion prefactor and activation energy from first-principles and to further investigate their trend in diffusivities and their magnetic nature.

Over the past quarter century, many experimental studies<sup>6–22</sup> have been conducted to measure the diffusion coefficients of 3d transition elements in Al. From the measurements it had been observed that compared to Al self-diffusion, diffusivities of 3d elements is *anomalously* low, resulting from high diffusion prefactor  $D_0$  and high activation barrier  $Q$ , though the cause for such a behavior is not clear. In the present work an attempt is made to understand the cause for the anomalously low diffusion coefficients of 3d solutes in Al from existing theories.

### II. THEORY

Impurity diffusion coefficient for a cubic system is expressed in the Einstein form as<sup>23</sup>

$$D_2 = f_2 a^2 C_2 w_2, \quad (1)$$

where  $a$  is the lattice parameter,  $f_2$  is the solute diffusion correlation factor,  $C_2$  is the vacancy concentration adjacent to the solute, and  $w_2$  is the solute jump frequency. We employ the five-frequency model of Le Claire<sup>23</sup> to compute the solute correlation factor  $f_2$  for dilute fcc alloys as derived by Manning<sup>24</sup>

$$f_2 = \frac{1 + 3.5F(w_4/w_0)(w_3/w_1)}{1 + (w_2/w_1) + 3.5F(w_4/w_0)(w_3/w_1)},$$

where

$$F(x) = 1 - \frac{1}{7} \frac{10x^4 + 180.5x^3 + 927x^2 + 1341}{2x^4 + 40.2x^3 + 254x^2 + 597x + 435} \quad (2)$$

$x = w_4/w_0$  and  $w_i$  are the five jump frequencies:  $w_1$  represents jumps of solvent atom adjacent to impurity with the vacancy adjacent to impurity before and after the jump,  $w_4$  represents jumps of solvent atom such that vacancy associates with or comes adjacent to the impurity atom,  $w_3$  represents jump of solvent atom such that vacancy disassociates with the impurity atom,  $w_0$  is the jump of solvent atom, without vacancy or the diffusing solvent atom being adjacent to impurity before and after the jump (jump frequency in pure solvent system) and  $w_2$  is the jump of the solute atom with adjacent vacant site.

Atom jump frequency can be described by the equation<sup>25</sup>

$$w = \frac{k_B T}{h} \exp\left(-\frac{G_{\text{TS}}^* - G_{\text{IS}}}{k_B T}\right), \quad (3)$$

where  $G_{\text{IS}}$  is the free energy of the initial state (IS) of a system with a vacancy and all the atoms in their equilibrium positions and  $G_{\text{TS}}^*$  is the free energy of the transition state (TS) with the diffusing atom at the saddle point along the diffusion path, after excluding the contribution from its unstable phonon mode.

The vacancy concentration  $C_2$  is defined from the probability of vacancy formation adjacent to an impurity atom<sup>26</sup>

$$C_2 = \exp\left(-\frac{\Delta G_f}{k_B T}\right), \quad (4)$$

where  $\Delta G_f = \Delta G_f^\circ - \Delta G_b$  with  $\Delta G_f^\circ$  being the free energy of vacancy formation in pure solvent without impurity and  $\Delta G_b$  being the solute-vacancy binding energy<sup>27</sup> defined as  $\Delta G_b = -(G_{\text{IS}}^{w_1} - G_{\text{IS}}^{w_4})$ , i.e., negative of the difference between free energies of the system when solute and vacancy are adjacent to each other ( $w_1$  jump) and when they are apart ( $w_4$  jump). Thus calculating the impurity diffusion coefficient is reduced to obtaining the temperature-dependent enthalpy and entropy of the pure solvent without vacancy and of the initial and

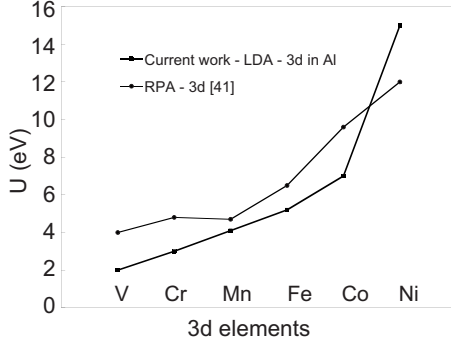


FIG. 1. Hubbard  $U$  from the current work in comparison to values from the work of Aryasetiawan *et al.* (Ref. 41).

transition states corresponding to the five jumps. It is noted from the five-frequency model that the initial states of jumps  $w_1$ ,  $w_2$ , and  $w_3$ , and the transition states of  $w_3$  and  $w_4$  jumps are the same.<sup>27</sup>

Considering the temperature dependence of  $f_2$  which contributes to the activation energy of impurity diffusion coefficient, with jump frequencies involving terms of the form  $\exp(1/k_B T)$ , Eq. (1) in the Arrhenius' form  $D = D_0 \exp(-Q/k_B T)$  can be written as

$$D_2 = \frac{\frac{k_B T}{h} f_2 a^2 \exp\left(\frac{S_{TS}^* - S_{IS}^{w_4} + \Delta S_f^o}{k_B}\right)}{\exp\left[\frac{k_B d \ln f_2/d(1/T)}{k_B T}\right]} \times \exp\left[-\frac{H_{TS}^* - H_{IS}^{w_4} + \Delta H_f^o - k_B d \ln f_2/d(1/T)}{k_B T}\right],$$

where the activation energy is

$$Q = H_{TS}^* - H_{IS}^{w_4} + \Delta H_f^o - k_B d \ln f_2/d(1/T). \quad (5)$$

TABLE I. Activation energies for 3d elements in Al obtained using LDA and LDA+ $U$  with and without spin polarization. The  $U$ - $J$  values used in the LDA+ $U$  calculations are listed. Activation energy of the Al-3d system from suitable type of potential is shown in bold. Assessed experimental data for activation energy is tabulated for comparison. All the values listed in the table are in eV.

3d element	$U$ - $J$	$Q$ (LDA+ $U$ +spin)	$Q$ (LDA+ $U$ +non-spin)	$Q$ (LDA+spin)	$Q$ (LDA+nonspin)	$Q$ (Exp)	Exp References
Sc	1	1.69	1.69		<b>1.72</b>	1.79	42
Ti	1	2.31	2.31		<b>2.34</b>	2.71	43
V	1	<b>2.50</b>	2.64		2.63	3.14	43
Cr	2	<b>2.08</b>	2.79	2.81		2.71	44
Mn	3	<b>1.65</b>	2.82	2.79		2.19	44
Fe	4	<b>1.40</b>	2.59	2.55		2.00	12
Co	6	2.10	<b>1.23</b>	2.22		1.75	44
Ni	14	1.57	<b>1.30</b>	1.75		1.50	44
Cu	9	1.22	1.22		<b>1.25</b>	1.39	44
Zn	9	1.18	1.18		<b>1.17</b>	1.20	44

### III. CALCULATION METHODOLOGY

In the present work, the first-principles calculations are performed using the projector-augmented wave (PAW) method,<sup>28,29</sup> as implemented in the highly efficient Vienna *ab initio* simulation package (VASP).<sup>30</sup> The LDA (Ref. 31) is used for the exchange-correlation potential. A Monkhorst-Pack  $k$ -point mesh of  $8 \times 8 \times 8$  and energy cutoff of 300–350 eV depending on the valence description of the pseudopotential yielded converged migration barriers within 0.01 eV. Similar convergence of the energetics was obtained using supercells with 32 and 64 lattice sites. Hence supercell with 32 lattice sites ( $2 \times 2 \times 2$  fcc supercell) was employed. Unless otherwise mentioned, all calculations are completely relaxed with respect to internal coordinates, volume, and shape. The transition state is determined by the nudged elastic band method<sup>32</sup> as implemented by VASP.

The phonon frequencies are calculated using the supercell approach,<sup>33</sup> as implemented in the alloy theoretic automated toolkit (ATAT) (Ref. 34) package. Similar energy cut-off and  $k$ -point mesh sizes used for the static total energies are also used for the vibrational calculations. The contributions to the free energy from the normal phonon frequencies are calculated through the standard thermodynamic relations.<sup>35</sup> From our previous work<sup>36</sup> it has been observed that temperature dependences due to thermal expansion are negligible for Al. Hence in the present work calculations are performed within the harmonic approximation<sup>37</sup> at the fixed 0 K equilibrium volume for the initial and transition states.

Using the PAW method or ultrasoft (US) pseudopotential together with LDA for obtaining the relaxed configurations of the transition state, specifically for Cr, Mn, Fe, Co, and Ni impurities, the spin-polarized calculation exhibited magnetic moment irregularly, causing huge deviations in the energetics on the order of 0.5 eV. Allowing only constrained relaxation, i.e., relaxing the atom positions without changing the volume or cell shape, a procedure similar to that followed by Sandberg and Holmestad,<sup>2</sup> stabilized the energetics and improved the activation energy in comparison to experiments for some of these impurities while others remained almost unaffected.

TABLE II. Magnetic moments ( $\mu_B$ ) of the fully relaxed perfect, initial and transition states of the impurity jump, obtained from LDA +  $U$  relaxation using  $J=1$  eV and  $U$ - $J$  values from column 2 of Table I, in comparison with results from experimental measurement and predictions from other theories in the literature.

3d element	Magnetic moment						
	Perfect state		Initial state (LDA+ $U$ )	Transition state (LDA+ $U$ )	Experiments	Theories	References
	(LDA+ $U$ )	LDA					
V	0.02	0.0	0.0	2.1			
Cr	3.03	0.11	3.10	3.76		2.00	45
						2.8	46
Mn	3.33	0.0	3.39	3.95		2.53	45
						2.46	47
						2.4	46
Fe	2.26	0.00	2.38	2.88	0 <sup>a</sup>	1.78	45
						0.6	46
						1.9	4
Co	0.85	0.0	1.3	1.3			
Ni	0.0	0.0	0.0	0.0			

<sup>a</sup>References 48 and 49.

Thus, performing full or constrained relaxation using PAW LDA or US LDA potentials did not yield activation energies and impurity diffusion coefficients that consistently matched with experimental results. There exists a complication in handling Al systems with 3d transition metal solutes within LDA or DFT due to localization of charges around the transition-metal elements.<sup>38</sup> To treat such a case where both bandlike and localized behavior exists in dilute alloys with transition metals, LDA+ $U$  (Ref. 39) potential is proposed to include the electron-electron correlation and exchange energies of the partially filled  $d$  shell of the transition impurities within the Hamiltonian of the system through  $U$  and  $J$  parameters, respectively.

In this work, the Hubbard model implemented by VASP is used along with PAW LDA (LDA+ $U$ ) for modeling these metallic systems.<sup>40</sup> The Hubbard  $U$  for the 3d elements has been recently estimated (shown in Fig. 1) by Aryasetiawan *et al.*<sup>41</sup> using a random-phase-approximation (RPA) scheme. Using these  $U$  values as our initial guess, diffusion coefficients of all 3d elements have been calculated. The  $U$ - $J$  (where  $J=1$  eV) value is then adjusted and both spin-polarized and nonspin-polarized relaxations are conducted to obtain an appropriate description of the charge interactions in each Al-3d system, by comparing the predicted 3d diffusivities with experimental data. Analysis conducted of the experimental data in the literature for each Al-3d system has revealed that only few of the experimental works obtained consistent  $D_0$  values varying over a small range (about an order of magnitude) while the others obtained much higher or lower values. Measurements that yielded nearly consistent diffusion parameter values have been considered *reliable* in this work and chosen for comparison. The suitable  $U$ - $J$  value and spin-relaxation type for each Al-3d system and the resulting activation energy in comparison with experimental data are tabulated in Table I. Values obtained by Du *et al.*<sup>44</sup> from least-squares analysis, for 3d elements assessed from

reliable experimental data, have been used for comparison in Table I. For the other 3d elements reliable data of the available measurements are chosen. The  $U$  values from the current work are compared to those from the RPA work of Aryasetiawan *et al.*<sup>41</sup> in Fig. 1. The magnetic moments and partial density of states (DOS) from  $d$  orbital ( $d$ -DOS) of the transition elements are reported.

#### IV. RESULTS AND DISCUSSIONS

The correlation factor calculated from five-frequency model [Eq. (2)], for diffusion of all 3d impurities except Zn, is obtained to be *unity* at all temperatures considered, indicating uncorrelated motion of partially filled transition elements in Al. In such cases, activation energy [Eq. (5)] is just the sum of the enthalpy of vacancy formation and impurity migration (temperature dependence of impurity correlation factor is zero). The correlation factor for Zn diffusion increases from 0.06 to 0.53 with the temperature increasing from 400 to 900 K. This temperature dependence of the correlation factor [see Eq. (5)] contributes a value of 0.14 eV in addition to the sum of enthalpy of vacancy formation and atom migration for the activation energy of Zn.

For comparison of the activation energies from the current work to experimental data, assessed values of Du *et al.*<sup>44</sup> and data consistent over different works of measurements chosen, are tabulated in Table I. It is seen that spin-polarized calculation does not change the energetics of the system with Sc, Ti, Cu, or Zn impurity in Al (see Table I), besides giving a zero magnetic moment on full relaxation, indicating the nonmagnetic nature of these dilute Al alloys. It is also found that an LDA+ $U$  calculation of activation energy in these alloys yields almost the same value as that from LDA, indicating low  $d$ - $d$  interactions for Sc and Ti with lower number of  $d$  electrons and also for Cu and Zn with completely filled  $d$  shell.

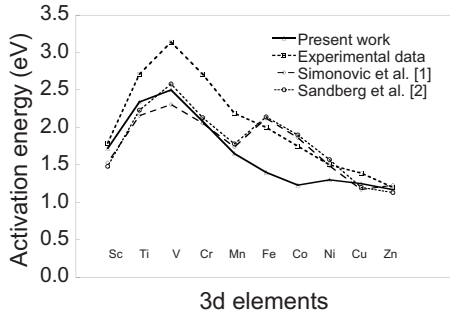


FIG. 2. Systematic match in the trend of activation energies between current work (LDA+ $U$ ) and experimental data (references in Table I). First-principles calculation results from Sluiter and co-workers (Ref. 1) and Sandberg and Holmestad (Ref. 2) are plotted for comparison.

For the case of solutes V to Ni, a significant change is seen in the energetics of the Al alloy system for a spin-polarized calculation (see columns 3 and 4 of Table I). The magnetic moments obtained from spin-polarized full relaxation of the three states (perfect state with no vacancy, and initial and transition states) of these Al-3d systems indicates that Fe, Cr, and Mn are magnetic, Ni and Co are nonmagnetic and V is magnetic when V is at the saddle point in transition state (see Table II). Comparing the LDA+ $U$  activation energies from spin-polarized calculations of V, Fe, Cr, and Mn, and nonspin-polarized calculations of Ni and Co solutes in Al, to assessed experimental data, a systematic agreement is seen (see Fig. 2 and Table I), indicating the importance in including the effective  $d$ - $d$  interaction energy ( $U$ - $J$ ). Further, it is seen that with increasing  $d$  electrons in the partially filled  $d$  shell, i.e., as we move across the 3d series from left to right, the  $U$ - $J$  value increases (see Fig. 1).

We attempt to understand the trend followed by the activation barriers of the 3d elements in Al, having a peak at V (see Fig. 2). Activation energies are not a function of solute excess valence or solute solubilities in Al.<sup>50</sup> The size of the 3d elements in fcc lattice varies across the series with a minimum at Fe.<sup>51</sup> Thus their activation energies are not a

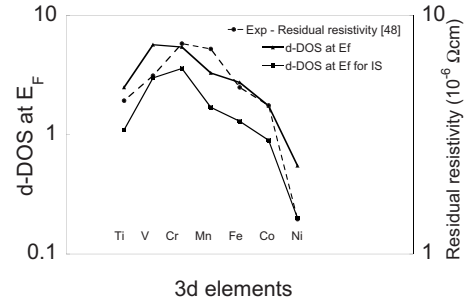


FIG. 3. Partial DOS from the  $d$  electrons of the transition element in Al at the Fermi level ( $E_F$ ) from nonspin-polarized fully relaxed IS and the sum of IS and perfect state (bold solid line). Residual resistivity values are taken from experimental work of Rizzuto (Ref. 53). Both the y axes are plotted on logarithmic scales.

function of their size either. Activation energy of 3d solute can be related to its bonding strength with its nearest-neighbor Al atoms, i.e., a combination of: (i) the bonding strength with Al in perfect state when there is no vacancy adjacent to the transition element, which determines the energy required for vacancy formation and, (ii) the bonding strength of the transition element with Al in initial state with a vacancy adjacent to it, which determines the energy for migration. Therefore, we analyze the total strength of bonding of each transition-metal impurity with its nearest neighbors before and after the formation of vacancy to understand the trend in their activation energies. In this respect, Morinaga *et al.*<sup>46</sup> also described the trend in activation barriers of 3d transition metal solutes in Al to be a function of bond strength.

According to the theory of *virtual bound state* proposed by Friedel<sup>52</sup> and Anderson to describe specifically the bonding of 3d impurity elements in Al, *resonance* between similar energy states of 3d element with Al causes scattering of the conduction electrons of Al, resulting in increased electronic density of states around the 3d element. As it is mainly the  $d$  electrons of the 3d element that are involved in bonding, we look at the partial density of states from the  $d$  orbital ( $d$ -DOS) of transition-metal impurity at the Fermi energy

TABLE III.  $Q$  and  $D_0$  values from the current work in comparison with experimental data.

3d element	$U$ - $J$	LDA+ $U$		Experiments		References
		$Q$ (eV)	$D_0$ (m <sup>2</sup> /sec)	$Q$ (eV)	$D_0$ (m <sup>2</sup> /sec)	
Sc	1	1.72	$5 \times 10^{-5}$	1.79	$5.31 \times 10^{-4}$	42
Ti	1	2.32	$9 \times 10^{-5}$	2.71	$1.12 \times 10^{-1}$	43
V	1	2.50	$1 \times 10^{-4}$	3.14	$1.6 \times 10^0$	43
Cr	2	2.07	$7 \times 10^{-5}$	2.71	$6.75 \times 10^{-1}$	44
Mn	3	1.73	$2 \times 10^{-5}$	2.19	$1.35 \times 10^{-2}$	44
Fe	4	1.51	$3 \times 10^{-5}$	2.00	$1.35 \times 10^{-2}$	12
Co	6	1.17	$1.6 \times 10^{-6}$	1.75	$1.93 \times 10^{-2}$	44
Ni	14	1.42	$2 \times 10^{-4}$	1.50	$4.1 \times 10^{-4}$	44
Cu	9	1.24	$6.1 \times 10^{-6}$	1.39	$4.44 \times 10^{-5}$	44
Zn	9	1.2	$7 \times 10^{-6}$	1.20	$1.19 \times 10^{-5}$	44

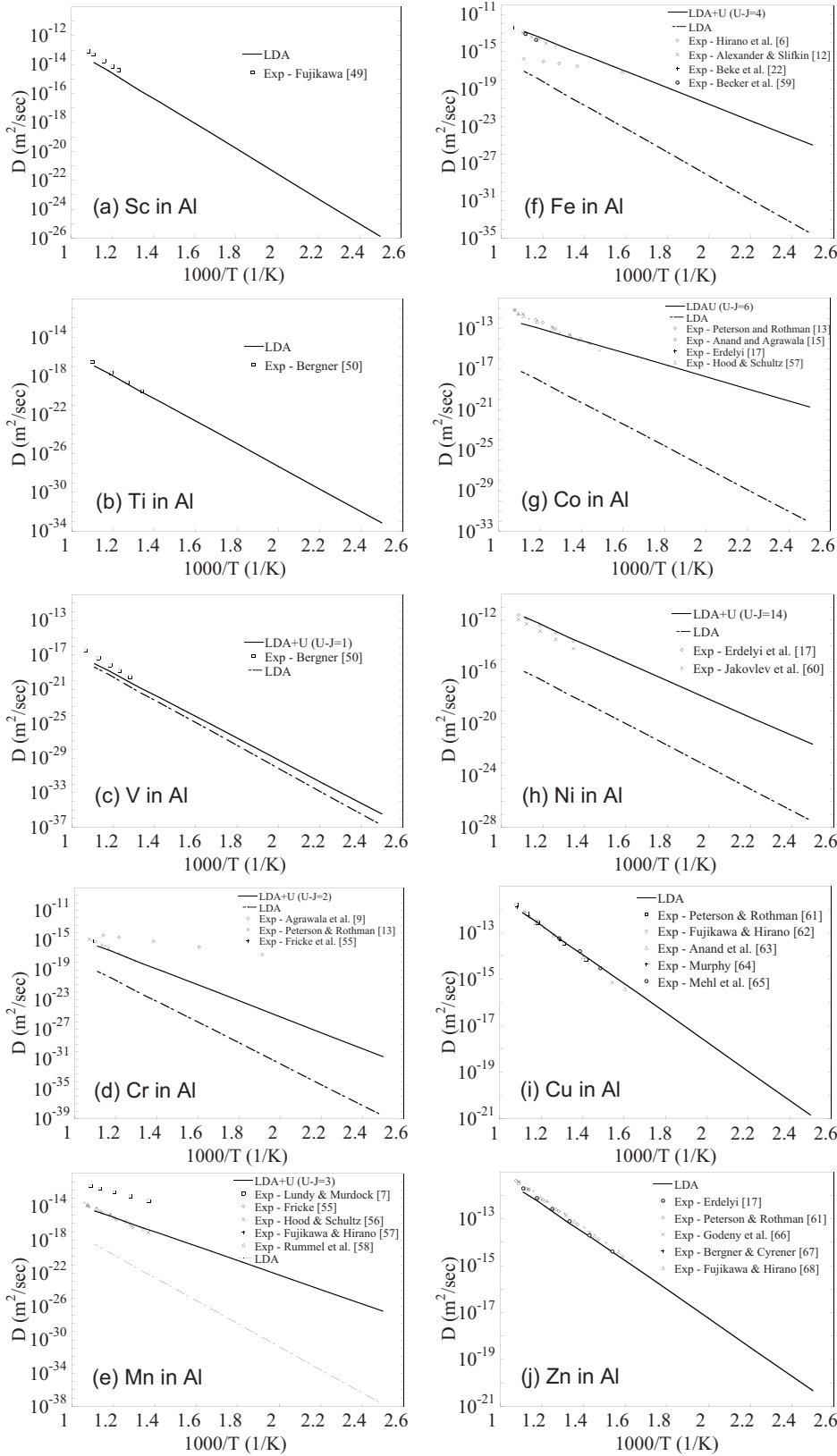


FIG. 4. Impurity diffusion coefficient from LDA and LDA+*U* (for systems required) in comparison with experimental data available in the literature for (a) Sc in Al (Ref. 42), (b) Ti in Al (Ref. 43), (c) V in Al (Ref. 43), (d) Cr in Al (Refs. 9, 13, and 55), (e) Mn in Al (Refs. 7 and 55–58), (f) Fe in Al (Refs. 6, 12, 22, and 59), (g) Co in Al (Refs. 13, 15, 17, and 57), (h) Ni in Al (Refs. 17 and 60), (i) Cu in Al (Refs. 61–65), and (j) Zn in Al (Refs. 17, 61, and 66–68).

level ( $E_F$ ) of the Al system. The sum of *d*-DOS of transition metal impurity in perfect and initial state is treated as a measure of the total (before and after formation of vacancy) bonding strength of the 3*d* element leading to its activation barrier. Resulting *d*-DOS values for elements across the 3*d*

period (plotted in Fig. 3) is a single-peak curve, with the peak at V, similar to the plot of activation energy (Fig. 2). Additionally, according to the Friedel-Anderson theory, greater the electronic density of states around the 3*d* element<sup>54</sup> greater should be the residual electrical resistivity



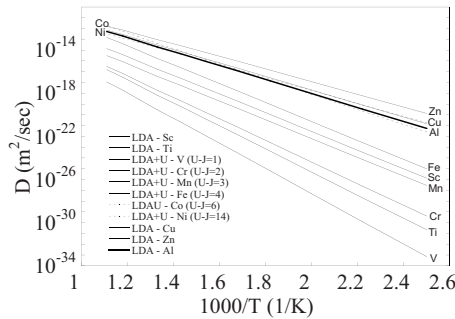


FIG. 5. Figure 5 illustrates the nonanomalous diffusion behavior of Co and Ni in Al, in contrast to *anomalous* behavior of all other 3d transition elements with partially filled  $d$  shell.

of the Al-3d system. Following similar concept, Sandberg *et al.*<sup>2</sup> explained higher diffusion barriers of the midseries 3d elements in Al to be the effect of greater electronic scattering (related to higher residual resistivity) caused by these impurities in Al. As  $d$ -DOS of perfect state at  $E_F$  [V(2.7) > Cr(1.85) > Mn(1.6) > Fe(1.45)] follows the same trend as the sum total  $d$ -DOS plotted in Fig. 3 we plot the resistivity data from measurements<sup>53</sup> in Fig. 3. It can be seen that the trends agree very well, thus proving the occurrence of *resonance* and *conduction electron-scattering* phenomena in bonding between Al and 3d. It is also seen from Figs. 2 and 3 that the trend in activation energy for all elements across the 3d series is not explainable on the basis of  $d$ -DOS at  $E_F$  itself and hence there could be contributions from other secondary factors.

As can be seen from the magnetic moments obtained from the present calculations (see Table II), dilute Al alloy with Fe, Cr, or Mn impurity is magnetic, even in its fully relaxed state, unlike claims by previous researchers.<sup>3-5</sup> Magnetic nature is also evident from the distinct two-peaked (spin-up and spin-down) partial DOS from the  $d$  orbital of Fe, Cr, and Mn unlike other 3d elements.

$D_0$  and  $Q$  values calculated for all 3d transition elements' diffusion in Al are given in Table III. Impurity diffusion coefficients obtained from these values are illustrated in Fig. 4. The results from both LDA and LDA+ $U$  are plotted for systems where the  $U$ - $J$  parameter has a significant impact. On comparing the diffusion coefficients of all the 3d elements in Al in Fig. 5, we see that the trend in diffusivity of 3d elements closely follows the trend in their activation energy (Fig. 2). On comparison of diffusion coefficients of 3d elements with Al self-diffusion<sup>36</sup> (see Fig. 5), it can be seen that 3d elements Sc to Fe exhibit *anomalously* low diffusion coefficients compared to Al self-diffusion. We expect their low diffusivities and high activation barriers in Al to be due to strong bonding with Al, a consequence of increased electron density from Friedel-Anderson's *virtual bound state*. In this

context, Simonovic *et al.*<sup>1</sup> also explained the anomalously high activation barriers of the midseries 3d elements to be due to strong bonding arising from  $sp$ - $d$  electronic hybridization between Al and the 3d solute elements. In the case of Co and Ni, due to large  $d$ - $d$  interactions causing highly localized charges as indicated by their significantly large  $U$ - $J$  values (Fig. 1) and low  $d$ -DOS (Fig. 3), the effect of *resonance scattering* is minimal, leading to small activation energies and thus *normal* diffusivities in Al, i.e.,  $\sim 2$ - $3$  orders of magnitude about Al self-diffusion. Similarly Cu and Zn with completely filled  $d$  shell do not have their  $d$  electrons actively participating in bonding with Al and hence exhibit *normal* diffusivities.

## V. CONCLUSIONS

In the present work, we found that LDA+ $U$  is suitable for describing the finite temperature energetics in Al-3d systems. This we see from the activation barriers and diffusion prefactors that systematically agree with measurements and, diffusion coefficients that match well with experimental data. Trend followed by the DOS from  $d$  orbital of 3d elements at Fermi level being similar to the residual resistivity data from experiments, shows occurrence of Friedel Anderson's *resonance-scattering* phenomenon for bonding between Al and 3d elements. Behavior of 3d solutes with their activation energy following similar pattern as their partial density of states at the Fermi level, with a peak at V, indicates strong correlation between their activation energies and the nature of bonding of 3d with Al as described by Friedel.<sup>36</sup> High activation barriers and *anomalously* low diffusion coefficients, for partially filled  $d$ -shell 3d elements, reflect strong bonding of 3d elements with Al. Exceptions to this are Co and Ni with high  $d$ - $d$  interactions and thus weak bonding with Al. Further it is seen that Al with dilute concentration of Cr, Mn, or Fe impurity is magnetic.

## ACKNOWLEDGMENTS

This work is funded by the National Science Foundation (NSF) under Grants No. DMR-0510180 and No. DMR-0205232. First-principles calculations were carried out on the LION clusters at the Pennsylvania State University supported in part by the NSF under Grants No. DMR-9983532 and No. DMR-0122638, and in part by the Materials Simulation Center and the Graduate Education and Research Services at the Pennsylvania State University. Calculations were also carried out on the INTI clusters from the computer science department at Pennsylvania State University supported by NSF under Grant No. CISE-0202007. Resources at NCSA via NSF under Grant No. DMR-070055N were used for testing 64 atom supercell calculations.

- <sup>1</sup>D. Simonovic and M. H. F. Sluiter, Phys. Rev. B **79**, 054304 (2009).
- <sup>2</sup>N. Sandberg and R. Holmestad, Phys. Rev. B **73**, 014108 (2006).
- <sup>3</sup>F. Lechermann, M. Fahnle, B. Meyer, and C. Elsasser, Phys. Rev. B **69**, 165116 (2004).
- <sup>4</sup>P. G. Gonzales, L. A. Terrazos, H. M. Petrilli, and S. Frota-Pessoa, Phys. Rev. B **57**, 7004 (1998).
- <sup>5</sup>N. Papanikolaou, R. Zeller, P. H. Dederichs, and N. Stefanou, Comput. Mater. Sci. **8**, 131 (1997).
- <sup>6</sup>K.-I. Hirano, R. P. Agarwala, and M. Cohen, Acta Metall. **10**, 857 (1962).
- <sup>7</sup>T. S. Lundy and J. F. Murdock, J. Appl. Phys. **33**, 1671 (1962).
- <sup>8</sup>R. W. Balluffi, Acta Metall. **11**(9), 1109 (1963).
- <sup>9</sup>R. P. Agarwala, S. P. Murarka, and M. S. Anand, Acta Metall. **12**, 871 (1964).
- <sup>10</sup>S. P. Murarka, M. S. Anand, and R. P. Agarwala, Acta Metall. **16**, 69 (1968).
- <sup>11</sup>G. M. Hood, Philos. Mag. **21**, 305 (1970).
- <sup>12</sup>W. B. Alexander and L. M. Slifkin, Phys. Rev. B **1**, 3274 (1970).
- <sup>13</sup>N. L. Peterson and S. J. Rothman, Phys. Rev. B **1**, 3264 (1970).
- <sup>14</sup>R. S. Preston and R. Gerlach, Phys. Rev. B **3**, 1519 (1971).
- <sup>15</sup>M. S. Anand and R. P. Agarwala, Philos. Mag. **26**, 297 (1972).
- <sup>16</sup>A. Tonejc, Philos. Mag. **27**, 753 (1973).
- <sup>17</sup>G. Erdélyi, D. L. Beke, F. J. Kedves, and I. Gödény, Philos. Mag. B **38**, 445 (1978).
- <sup>18</sup>S. Mantl, W. Petry, K. Schroeder, and G. Vogl, Phys. Rev. B **27**, 5313 (1983).
- <sup>19</sup>D. L. Beke, I. Godeny, G. Erdelyi, and F. J. Kedves, Mater. Sci. Forum **13-14**, 519 (1987).
- <sup>20</sup>S. Fujikawa and K. Hirano, Mater. Sci. Forum **13-14**, 539 (1987).
- <sup>21</sup>B. S. Bokstein, Mater. Sci. Forum **217-222**, 685 (1996).
- <sup>22</sup>D. L. Beke, I. Godeny, G. Erdelyi, F. J. Kedves, and J. Felszerfalve, Defect Diffus. Forum **66-69**, 427 (1990).
- <sup>23</sup>A. D. Le Claire, J. Nucl. Mater. **69-70**, 70 (1978).
- <sup>24</sup>J. R. Manning, Phys. Rev. **136**, A1758 (1964).
- <sup>25</sup>N. L. Peterson, J. Nucl. Mater. **69-70**, 3 (1978).
- <sup>26</sup>R. E. Howard and A. B. Lidiard, Rep. Prog. Phys. **27**, 161 (1964).
- <sup>27</sup>M. Mantina, Y. Wang, L. Q. Chen, Z. K. Liu, and C. Wolverton, Acta Mater. **57**, 4102 (2009).
- <sup>28</sup>P. E. Blochl, Phys. Rev. B **50**, 17953 (1994).
- <sup>29</sup>G. Kresse and D. Joubert, Phys. Rev. B **59**, 1758 (1999).
- <sup>30</sup>G. Kresse and J. Furthmuller, Phys. Rev. B **54**, 11169 (1996).
- <sup>31</sup>D. M. Ceperley and B. J. Alder, Phys. Rev. Lett. **45**, 566 (1980).
- <sup>32</sup>G. Henkelman and H. Jonsson, J. Chem. Phys. **113**, 9978 (2000).
- <sup>33</sup>S. Wei and M. Y. Chou, Phys. Rev. Lett. **69**, 2799 (1992).
- <sup>34</sup>A. Van de Walle, M. Asta, and G. Ceder, CALPHAD: Comput. Coupling Phase Diagrams Thermochem. **26**, 539 (2002).
- <sup>35</sup>Y. Wang, Z.-K. Liu, and L.-Q. Chen, Acta Mater. **52**, 2665 (2004).
- <sup>36</sup>M. Mantina, Y. Wang, R. Arroyave, L. Q. Chen, Z. K. Liu, and C. Wolverton, Phys. Rev. Lett. **100**, 215901 (2008).
- <sup>37</sup>A. Van de Walle and G. Ceder, Rev. Mod. Phys. **74**, 11 (2002).
- <sup>38</sup>J. Friedel, Nuovo Cimento, Suppl **7**, 287 (1958).
- <sup>39</sup>V. I. Anisimov, F. Aryasetiawan, and A. I. Lichtenstein, J. Phys.: Condens. Matter **9**, 767 (1997).
- <sup>40</sup>S. L. Dudarev, G. A. Botton, S. Y. Savrasov, C. J. Humphreys, and A. P. Sutton, Phys. Rev. B **57**, 1505 (1998).
- <sup>41</sup>F. Aryasetiawan, K. Karlsson, O. Jepsen, and U. Schonberger, Phys. Rev. B **74**, 125106 (2006).
- <sup>42</sup>S.-I. Fujikawa, Defect Diffus. Forum **143-147**, 115 (1997).
- <sup>43</sup>D. Bergner, Neue Hutte **29**, 207 (1984).
- <sup>44</sup>Y. Du, Y. A. Chang, B. Huang, W. Gong, Z. Jin, H. Xu, Z. Yuan, Y. Liu, Y. He, and F.-Y. Xie, Mater. Sci. Eng. **2003**, 140 (2003).
- <sup>45</sup>L. I. Kurkina, O. V. Farberovich, and V. A. Gorbunov, J. Phys.: Condens. Matter **5**, 6029 (1993).
- <sup>46</sup>M. Morinaga, S. Nasu, H. Adachi, J. Saito, and N. Yukawa, J. Phys.: Condens. Matter **3**, 6817 (1991).
- <sup>47</sup>R. M. Nieminen and M. Puska, J. Phys. F **10**, L123 (1980).
- <sup>48</sup>D. Riegel, L. Buermann, K. D. Gross, M. Luszik-Bhadra, and S. N. Mishra, Phys. Rev. Lett. **61**, 2129 (1988).
- <sup>49</sup>D. Guenzburger and D. E. Ellis, Phys. Rev. Lett. **67**, 3832 (1991).
- <sup>50</sup>W. G. Moffatt, *Handbook of Binary Phase Diagrams* (Genium, Schenectady, NY, 1978).
- <sup>51</sup>Y. Wang, S. Curtarolo, C. Jiang, R. Arroyave, T. Wang, G. Ceder, L.-Q. Chen, and Z.-K. Liu, CALPHAD: Comput. Coupling Phase Diagrams Thermochem. **28**, 79 (2004).
- <sup>52</sup>J. Friedel, in *Metallic Solid Solutions*, edited by J. Friedel and A. Guinier (W. A. Benjamin, New York, 1963), p. XIX.
- <sup>53</sup>C. Rizzuto, Rep. Prog. Phys. **37**, 147 (1974).
- <sup>54</sup>M. E. Lautenschläger and E. Mrosan, Phys. Status Solidi B **91**, 109 (1979).
- <sup>55</sup>W. G. Fricke, in *American Society for Metals*, edited by K. R. van Horn, (Metals Park, Ohio, 1967), Vol. 1.
- <sup>56</sup>G. Rummel, T. Zumkley, M. Eggersmann, K. Freitag, and H. Mehrer, Z. Metallkd. **85**, 122 (1995).
- <sup>57</sup>G. M. Hood and R. J. Schultz, Philos. Mag. **23**, 1479 (1971).
- <sup>58</sup>S. Fujikawa and K. Hirano, Mater. Sci. Eng. **27**, 25 (1977).
- <sup>59</sup>C. Becker, G. Erdelyi, G. M. Hood, and H. Mehrer, Defect Diffus. Forum **66-69**, 409 (1990).
- <sup>60</sup>S. G. Yakovlev, E. I. Mozzhukhin, and P. B. Smirnov, Izv. Vyssh. Uchebn. Zaved., Tsvetn. Metall. **4**, 145 (1974).
- <sup>61</sup>N. L. Peterson and S. J. Rothman, Phys. Rev. B **17**, 4666 (1978).
- <sup>62</sup>S. Fujikawa and K. Hirano, Defect Diffus. Forum **66-69**, 447 (1990).
- <sup>63</sup>M. S. Anand, S. P. Murarka, and R. P. Agarwala, J. Appl. Phys. **36**, 3860 (1965).
- <sup>64</sup>J. B. Murphy, Acta Metall. **9**, 563 (1961).
- <sup>65</sup>R. H. Mehl, F. N. Rhines, and K. A. Vonden Steinen, Met. Alloys **13**, 41 (1941).
- <sup>66</sup>I. Gödény, D. L. Beke, and F. J. Kedves, Phys. Status Solidi A **13**, K155 (1972).
- <sup>67</sup>D. Bergner and E. Cyrener, Neue Hutte **18**, 356 (1973).
- <sup>68</sup>S. Fujikawa and K.-I. Hirano, Trans. Jpn. Inst. Met. **17**, 809 (1976).